Evaluation of the PANS method for the prediction of the fluid flow in a cyclone separator

Zaher Bitar, David Uystepruyst, François Beaubert, Damien Méresse, Céline Morin

INSTITUT DE FRANCE
Académie des sciences

Comptes Rendus
Mécanique

Zaher Bitar, David Uystepruyst, François Beaubert, Damien Méresse and Céline Morin

Evaluation of the PANS method for the prediction of the fluid flow in a cyclone separator

Volume 351 (2023), p. 201-218

Published online: 25 May 2023

https://doi.org/10.5802/crmeca.186

Les Comptes Rendus. Mécanique *sont membres du Centre Mersenne pour l'édition scientifique ouverte*
www.centre-mersenne.org
e-ISSN : 1873-7234

Comptes Rendus
Mécanique
2023, Vol. 351, p. 201-218
https://doi.org/10.5802/crmeca.186

Spontaneous Articles / *Articles spontanés*

Evaluation of the PANS method for the prediction of the fluid flow in a cyclone separator

Zaher Bitar [a], David Uystepruyst [a], François Beaubert [a], Damien Méresse [a] and Céline Morin [a]

[a] LAMIH UMR CNRS 8201, Le Mont-Houy, 59313 Valenciennes CEDEX 9, France
E-mails: zaher.bitar@uphf.fr (Z. Bitar), david.uystepruyst@uphf.fr (D. Uystepruyst), francois.beaubert@uphf.fr (F. Beaubert), damien.meresse@uphf.fr (D. Méresse), celine.morin@uphf.fr (C. Morin)

Abstract. The simulation of the cyclone separation efficiency can rapidly become very expensive in time of calculation, which is not suitable for industrial application. The prediction of the complex turbulent gas flow inside a cyclone is necessary to estimate its pressure drop, its characteristics and finally its separation efficiency. Even though classic models such as RSM and LES can effectively predict such type of flow, the quality of the results and the computation cost can be discussed. In this work, Partially Averaged Navier–Stokes (PANS) method is proposed to simulate the fluid flow inside a gas cyclone. Compared to experimental and numerical results of a literature review, this model predicts reasonably the time-averaged tangential and axial velocity fields, and more accurately the pressure drop across the cyclone in shorter CPU times. The sensitivity of the PANS approach to the unresolved to total kinetic energy ratio f_k was also evaluated with two different definitions. The first one was the standard definition developed by Girimaji et al. [1] and the second one was based on a statistical equivalence between the DES and PITM. The proposed model offers a better cost to quality ratio compared to the classic RANS approach.

Keywords. Cyclone, Industrial air cleaning, CFD, PANS, Turbulence.

Manuscript received 29 November 2022, revised 17 February 2023 and 22 March 2023, accepted 20 March 2023.

1. Introduction

Nowadays, air quality and particulate matter (PM) emission are subjected to stricter specifications that are assigned by laws. As one of many gas-solid separation techniques, gas cyclones are used to separate dust particles from the flue gases by means of centrifugal forces. They can be integrated on a wide variety of chemical and industrial processes. They are relatively simple to manufacture, to maintain and do not contain moving parts. All of this make the gas cyclones of substantial industrial importance and raise the interests of developing and optimizing them.

The key to optimizing a cyclone performance is to have a deep understanding of its 3D complex flow and the fluid-particles interaction. Computational Fluid Dynamics (CFD) approach

is often used to predict the velocity and pressure fields of the fluid flow and the Lagrangian fields for the discrete phase.

A lot of work has been done in this domain, especially when it comes to turbulence modelling. For high swirl intensity and anisotropic flows, first order RANS (Reynolds Average Navier Stokes) models such as $k-\varepsilon$, $k-\omega$ fail in modelling such flows, as highlighted by Boysan et al. [2]. Jafari et al. [3] compared the standard $k-\varepsilon$ turbulence model, the standard $k-\omega$ and SST with a curvature correction, the SSG RSM (Reynolds Stress Model) and the LES (Large Eddy Simulation) Smagorinsky models. They concluded that all models were able to predict the flow field inside the cyclone, except the standard version of $k-\varepsilon$ turbulence model. The modified SST needed a low Reynolds treatment with a $y^+ = 2$. The standard $k-\varepsilon$ model was found in good agreement with the tangential velocities, while this model failed to predict the axial velocities. Hoekstra et al. [4] compared the standard $k-\varepsilon$, the RNG $k-\varepsilon$ turbulence models to the experimental data investigated in cyclone separator. They found out that these two models are not suited for swirling flows because they fail to reproduce the tangential and axial velocity distributions of the flow. In order to capture the anisotropy of the flow, they also tried a second order closure turbulence model, the RSM. The latter model was in good agreement with some LDA measurements. Bogdanov et al. [5] used a modified version of the $k-\omega$ SST model for the prediction of cyclone separation efficiency. They added a curvature correction term to enhance the prediction of the streamlines curvature.

Many authors [6–14] used the RSM for the cyclone flow and separation efficiency predictions. Jang et al. [15] compared the performances of the RSM and LES models to the experimental results. They concluded that RSM and LES models were both good at evaluating the fluid flow, while LES showed better accuracy. They also studied the influence of the turbulent dispersion on the separation efficiency by testing the flow with and without stochastic dispersion. The isotropic and anisotropic CRW and DRW (Continuous and Discrete Random Walk) approaches were tested in combination of the used turbulence models. They found out that the DRW is more accurate and specially when it is combined to LES. Elsayed et al. [16] used LES approach to study the fluid flow characteristics in the cyclone. LES approach was also in good agreement with experimental data. Gronald et al. [17] compared the flow field in the cyclone using finite volume RANS (RSM turbulence model), finite volume LES and Lattice Boltzmann LES. The LES approach showed better agreement with experimental data.

In the present work, the Partially Averaged Navier–Stokes (PANS) approach was implemented in OpenFOAM. Only a few articles discussed the use of this method for highly swirl and anisotropic flows and applications. For instance, Foroutan et al. [18] used PANS method for a swirling flow in an abrupt expansion. Comparisons were done with both experimental data and DDES results, and PANS was found to be closer to the experimental than DDES. But in fact it was proved to be superior over RANS and as effective as LES in many applications. Lakshmipathy et al. [19] have tested the PANS method while changing the viscosity reduction factor in a flow across a cylinder for a high Reynolds number and compared their results to those of LES [20] and some experimental results [21]. By decreasing the viscosity reduction factor the PANS results show a better precision. Indeed, the original version of the viscosity reduction factor is known to give too large value of turbulent viscosity vanishing all resolved turbulence, [18]. Lakshmipathy et al. [19] also compared the PANS to FSM method and some experimental data [22]. PANS predicted reasonably the mean streamwise velocity and the reattachment length. Further work was done on complex flow and geometries such as bluff and Ahmed body, internal combustion engine, flow around a real 3D car and crosswind on a moving rectangular object [23–25].

In this work, the PANS method is a novel approach that will be used for the fluid flow modelling in a gas cyclone. This method can be considered to be more accurate, especially predicting the separation efficiency of the cyclone, since it takes into consideration the temporal

and spatial dynamics of the flow. This method will be evaluated by comparing the results with other typical models such as RSM and LES that are widely used in this type of applications and with some experimental data [4]. The geometry and meshes of the reference configuration, the numerical settings and the PANS approach will be presented. In the next part, the grid and statistical convergence of the simulations are discussed. Then the influence of the turbulent closure approach (PANS, RSM) and meshing strategy is analyzed by comparing the present results to the LES results of Jang et al. [15] and the experimental work of Hoekstra et al. [4]. A discussion is also conducted on the influence of the f_k parameter of the PANS model.

2. Model description and setting

2.1. *Gas flow modelling*

The gas flow inside the cyclone is considered to be unsteady, incompressible and isothermal. The air density and dynamic viscosity are respectively 1.2 $kg.m^{-3}$ and $1.807.10^{-5}$ $kg.m^{-1}.s^{-1}$. For turbulence modelling, two different approaches were tested in this study : the proven RSM model and the PANS method which is innovative for this type of application.

2.2. *PANS method*

The computation cost, the accuracy and the ease of use are the main motivations for the choice of a method to model a complex turbulent gas flow. Despite the fact that RANS approach has a relatively low computation cost, it is limited when it comes to represent the different physical scale structures. Especially when more precision is required as in flows with high swirl and anisotropy such as in cyclones. LES resolves the larger eddies and models the subgrid scales by the means of a spatial filter, but it needs extensive computation time and resources which makes it less relevant for industrial configurations. Here comes the role of the PANS method, to solve the large scale eddies with an acceptable computation cost. The hybrid PANS method has a resolution and cost-accuracy that ranges from a RANS closure to a DNS approach. The degree of modelling is controlled by the unresolved to total ratio of kinetic energy f_k and dissipation f_ε.

$$f_k = \frac{k_{un}}{k_{total}} \tag{1}$$

$$f_\varepsilon = \frac{\varepsilon_{un}}{\varepsilon_{total}} \tag{2}$$

In this work, the two equations $k-\varepsilon$ PANS closure model was used. The first equation deals with the unresolved kinetic energy k_{un} and the second deals with the unresolved dissipation ε_{un}. The parameter f_k in PANS method is the equivalent to the cut-off wave number λ in LES. The resolved quantities of kinetic energy f_k will vary according to the grid size, as defined by Girimaji et al. [1]:

$$f_k = \frac{1}{\sqrt{C_\mu}} \left(\frac{\Delta_{min}}{\Lambda} \right)^{\frac{2}{3}} \tag{3}$$

where

$$\Lambda = \frac{k^{\frac{3}{2}}}{\varepsilon} \text{ and } \Delta_{min} = \min(\Delta x_1, \Delta x_2, \Delta x_3) \tag{4}$$

with Δx_1,Δx_2,Δx_3 are the local grid sizes in the x_1, x_2, x_3 directions.

The value of C_μ in the $k-\varepsilon$ PANS model is the same as in the $k-\varepsilon$ RANS and is taken equal to 0.09, Δ is the local size of the grid, Λ is the Taylor turbulent scale. The lower the value of f_k is, the higher the resolved to total kinetic energy ratio is, which means a higher resolution.

Another expression of the f_k term will be discussed in this work. This formulation, is proposed by Davidson et al. [26] and its principle lies about imitating the DES as follows:

$$f_k = \max\left[0, \min\left(1, 1 - \frac{\psi - 1}{C_{\varepsilon 1} - C_{\varepsilon 2}}\right)\right] \tag{5}$$

with

$$\psi = \max\left(1, \frac{\Lambda}{C_{DES}\Delta_{max}}\right) \tag{6}$$

where $C_{\varepsilon 1}$, $C_{\varepsilon 2}$ and C_{DES} are constants and Δ_{max} is defined by:

$$\Delta_{max} = \max(\Delta x_1, \Delta x_2, \Delta x_3). \tag{7}$$

2.3. *Geometry and meshing*

The geometric configuration used in this work (see Figure 1) is identical to the one used by Jang et al. [15]. In their work, they computed the velocity profiles in three different planes of the cyclones using LES and RSM models and compared them to the LDA measurements of Hoekstra et al. [4] for a Stairmand cyclone having a characteristic length $D = 0.29\ m$.

The purpose of using the same geometry is to be able to compare the results from the $k-\varepsilon$ PANS model, the LES (which is not simulated in this work see [15]) and the RSM model with the experimental data from [4] using the same opensource OpenFOAM code.

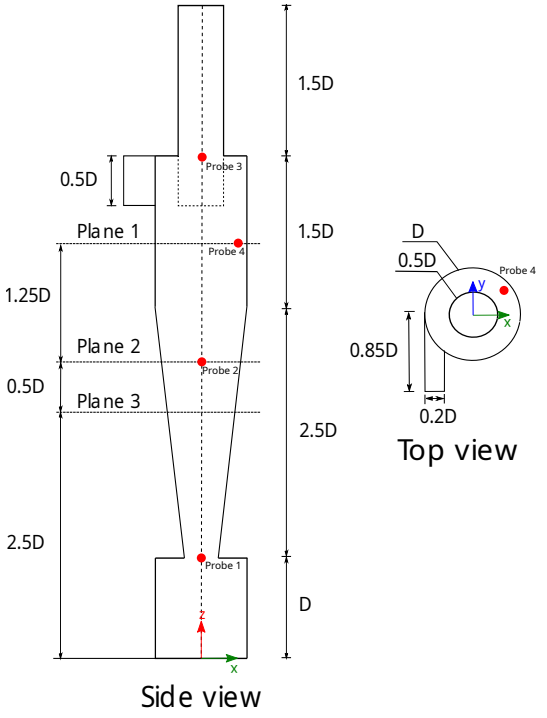

Figure 1. Cyclone's dimensions with the different planes/probes locations (characteristic length D = 0.29 m)

Three structured grids were created using `GMSH` open source mesher. Three other non-structured meshes where also generated using `snappyHexMesh` (see Table 1). Representations

of these meshes are shown in Figure 2. The average values of y^+ were 195, 180 and 152 for the RSM model on the coarse, the middle and the fine grid, respectively. For the PANS method, the average y^+ values were 209, 198 and 169.

Table 1. Characteristics of the grids.

Mesh	Mesh 1(coarse)	Mesh 2 (medium)	Mesh 3(fine)	Mesh 4 (coarse)	Mesh 5 (medium)	Mesh 6 (fine)
Number of cells	274 k	590 k	1 122 k	650 k	1 001 k	2 199 k
Type	structured	structured	structured	non-structured	non-structured	non-structured

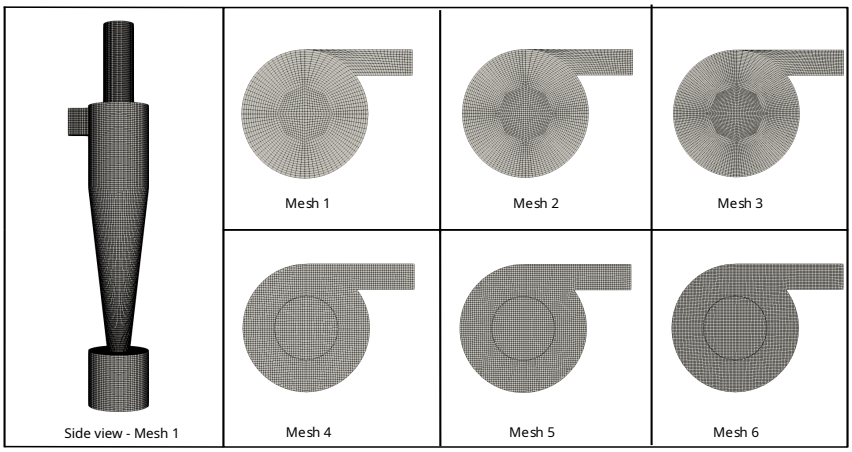

Figure 2. Side view and Z-cut representation of the 6 grids considered.

2.4. *Numerical settings*

Solver

The computation of the flow in the different cases was done by the `pimpleFoam` solver which consists of a combination of an incompressible and transient solvers. The same setup of the solver was used in all the cases. For $k-\varepsilon$ PANS and RSM models the second order interpolation scheme "linear upwind" was used for the continuity, the momentum equations and the turbulent variables. For the finest meshes cases with the $k-\varepsilon$ PANS model, the solution was initialized with the result of the intermediate mesh. For the RSM, the first order upwind interpolation scheme was applied to the Reynolds stress tensor. The time step was set to adjustable time step, while imposing a maximum value of $CFL = 1$.

Boundary conditions (BC)

For the sake of reproducibility, the inlet boundary conditions are similar to those of Jang et al. [15]. At the inlet the bulk velocity was set to 16.1 m/s, and the pressure gradient is set to zero. The turbulent kinetic energy was initialized by $k = \frac{3}{2}(UI)^2$, with a turbulence intensity I of 10%. The dissipation of the kinetic rate was initiated by $\varepsilon = c_\mu \frac{k^{\frac{3}{2}}}{l}$. Where the turbulent scale l is 0.07 times the width of the inlet. l was chosen instead of the hydraulic diameter in order to be coherent

with the study of Jang et al. [15]. The strong shear of the swirling flow in the cyclone will naturally trigger the turbulent instabilities of the flow.

For the outlet, a conditional BC was set for the velocity, zero-gradient is applied if the flux has a direction toward outside the cyclone, else the velocity is derived from patch-face normal component of the internal-cell value. For the pressure, a total pressure condition was set, where the value of pressure at patch face is equal to total pressure minus the dynamic pressure. This BC was used to avoid recirculation zones and negative velocity that are due to pressure difference between the outlet patch and the core region of the vortex finder. The turbulent kinetic energy and dissipation gradient were set to zero.

In order to prevent the numerical instabilities due to the transient nature of the problem, all the simulations were initialized by a RANS simulation using a realizable $k-\varepsilon$ turbulence model. These simulations were stopped once the solution at various probes locations in the cyclone became quasi-steady.

3. Results and discussion

In this work, the adopted methodology consists of comparing the results of cases simulated with $k-\varepsilon$ PANS and RSM models in this study, and the LES of Jang et al. [15] with respect to the experimental results of Hoekstra et al. [4]. The purpose of doing so is to evaluate the PANS method and compare it to other methods (RSM and LES) in modelling the fluid flow inside a cyclone. In order to estimate and compare the computational time with the $k-\varepsilon$ PANS model, the flow was solved in this work with the RSM turbulence model instead of using the results of the study of Jang et al. [15].

Table 3 summarizes the results of Normalized Mean Squared Difference (NMSD) for the velocity profiles and pressure drop for the calculations carried out in this study.

3.1. *The convergence criteria*

Iterative solution's convergence has been assessed according to solution imbalances. The iterative numerical solution process was considered to be converged once the residual values became at least inferior to 10^{-6}.

The mean solutions were considered to be statistically converged once the mean temporal velocity magnitude and pressure at several points became steady. An example of instantaneous velocities and pressures signals are presented in Figure 3, these latter signals were taken from the simulation of the case using the PANS model with the mesh 1 (coarse and structured).

The computation of the flow field using the PANS model was initialized with the realizable $k-\varepsilon$ solution at $t_0 = 3s$. The convergence time of the statistical means was about $2s$ of simulation for all the signals. The time averaging begun at $t_1 = 5s$ in order to have a faster establishment of the mean values by subtracting the effect of the signal overshoot. The same protocol was pursued for all the simulations cases. The time averaging of the flow fields was done until $t_2 = 7s$.

3.2. *The grid convergence index and sensitivity analysis*

In order to evaluate the grid convergence rate, the grid convergence index (GCI) was computed for the three structured meshes for both the RSM and $k-\varepsilon$ PANS turbulence models and the three unstructured meshes using only the $k-\varepsilon$ PANS model. The GCI method was used by Elsayed et al. [16, 27] to prove that their results are converging to an asymptotic range along with the refinement of the grid. This method is based on Richardson extrapolation that compares discrete

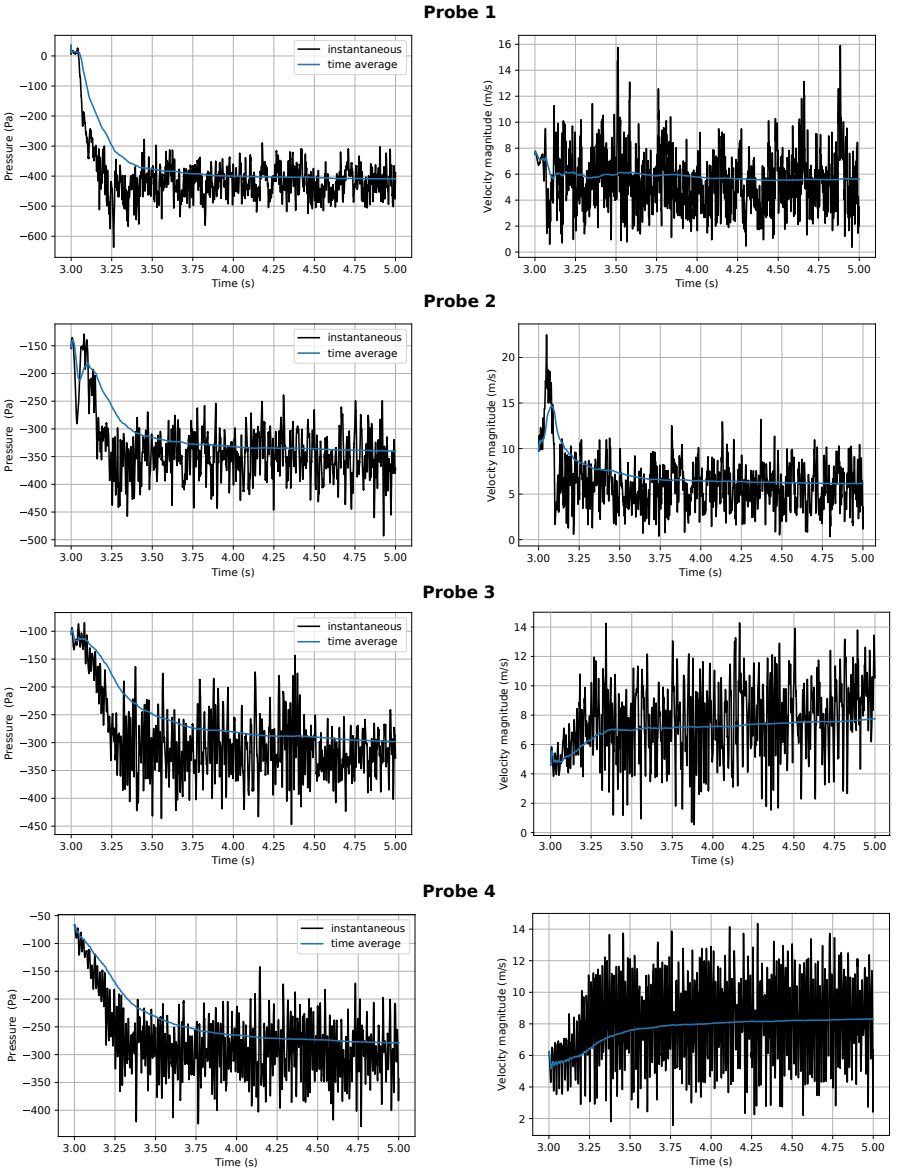

Figure 3. Statistical convergence of the pressure and the velocity at different probes locations (see Figure 1).

solution of two different grid sizes. The steps for the computation and further information of the GCI are found in the work of Roache and Elsayed et al. [14, 28]. Table 2 is the synthesis of these computations.

The parameter α shows the convergence behavior, ie. asymptotic or not. The values of α are equal to unity, which means that the solutions are converging to an asymptotic value for each case. In the case of the evaluation of the convergence rate for the three structured meshes using the $k-\varepsilon$ PANS turbulence model, the R value is smaller than unity which means that a monotonic convergence is reached. Meanwhile, using the RSM model with the structured and the $k-\varepsilon$ PANS model with the non-structured meshes, the R values are found to be superior to unity, which

Table 2. Computation of the convergence rate using GCI method.

ΔP	i	N_i	f_i	$r_{i,i+1}$	$e_{i,i+1}$	$\varepsilon_{i,i+1}$	$GCI^{fine}_{i,i+1}$%	R	α
RSM	0		627.8						
Mesh 3	1	1 122 544	682						
				1.239	21	0.03	-9.92		
Mesh 2	2	589 792	703					1.43	1.00
				1.290	15.1	0.021	-6.07		
Mesh 1	3	274 530	718.1						
$k-\varepsilon$ PANS	0		777.4						
Mesh 3	1	1 122 544	777.5						
				1.239	0.9	0.001	0.02		
Mesh 2	2	589 792	776.6					0.07	1.00
				1.290	11.7	0.015	0.16		
Mesh 1	3	274 530	764.9						
$k-\varepsilon$ PANS	0		821.7						
Mesh 6	1	2 199 229	938.5						
				1.299	-90.5	0.096	-16.5		
Mesh 5	2	1 001 076	1029.0					3.4	1.00
				1.152	-28.9	0.028	-4.4		
Mesh 4	3	653 429	1057.9						

means that the convergence is non-monotonic. The condition $GCI^{fine}_{1,2} < GCI^{fine}_{2,3}$ is also satisfied in the three cases. All of these conditions show that the solutions are tending asymptotically to the extrapolated values f_0, even if the convergence rate is non-monotonic with the latter two cases model. Ideally, one more fine grid could be used to see if the value of R decreases. But doubling the grid size in order to get a relatively small convergence will result in an important computational effort. According to the GCI method, the solutions can be considered as independent of the grid size.

To further characterize the sensitivity of the numerical solution to the mesh density, the time averaged axial and tangential velocity profiles were plotted in the three reference planes with

Table 3. NMSD of the velocity profiles at three axial positions and pressure drop for all the calculations.

Case		tangential velocity (%)			axial velocity (%)			pressure drop	
		P1	P2	P3	P1	P2	P3	Δp (Pa)	(%)
Experimental		-	-	-	-	-	-	773.1	-
mesh 1	RSM	0.9	0.6	0.5	5.9	8.1	14.9	718.1	-7.1
	PANS (eq. (3))	0.8	1.3	1.9	7.8	6.9	15.0	764.9	-1.1
mesh 2	RSM	1.8	1.4	1.8	5.6	8.0	14.8	703.0	-9.1
	PANS (eq. (3))	2.6	3.2	4.7	9.0	8.6	17.4	776.6	+0.5
mesh 3	LES [15]	1.2	3.0	0.7	18.3	6.6	20.7	691.7	10.5
	RSM	2.4	1.8	2.4	7.8	6.9	13.2	682	-11.8
	PANS (eq. (3))	4.0	4.6	6.6	11.1	10.6	21.4	777.5	+0.6
	PANS (eq. (5))	2.4	2.3	2.6	11.2	11.5	16.9	751.6	-2.8
mesh 4	PANS (eq. (3))	3.2	4.4	5.0	6.7	6.1	17.5	1057.9	+36.8
mesh 5	PANS (eq. (3))	6.1	7.4	8.3	8.6	6.3	16.4	1029.0	+33.1
mesh 6	PANS (eq. (3))	7.7	8.8	9.4	4.5	10.1	23.5	938.5	+21.4

respect to the experimental data [4]. Figures 4 and 5 represent the axial and tangential velocity profiles for the structured meshes 1, 2 and 3 for the RSM and $k-\varepsilon$ PANS respectively.

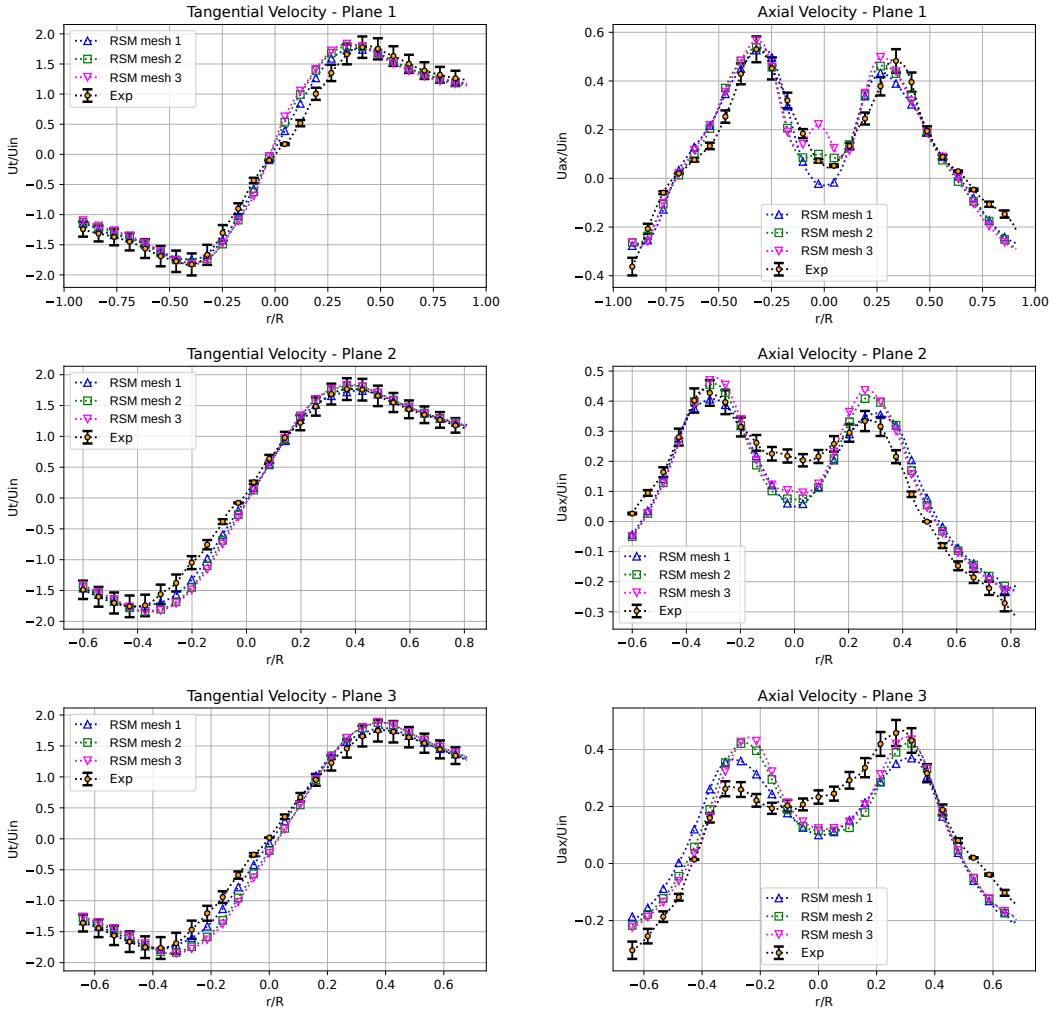

Figure 4. Radial distributions for the normalized mean tangential and axial velocities for the grids using the RSM turbulence model.

Figure 6 shows the comparison of the axial and tangential velocity profiles in the 3 planes for the unstructured meshes 4, 5 and 6 using the $k-\varepsilon$ PANS model. In order to quantify the differences relative to the experimental results [4] for the RSM and $k-\varepsilon$ PANS and for the different meshes, the NMSD are calculated and synthesized in Table 3. Figures and table show the increase of the percentages of difference for the tangential velocities with respect to the experimental results while refining the grids, which implies that the results are tending to the solutions for the 3 cases. In the other hand, the variation of the NMSD for the axial velocity does not have a clear tendency in the table. This could be explained by the fact that the axial velocities at fixed radial position are converging to the solution while refining the mesh, by having an increased or decreased difference value relatively to the experimental value. And for the overall radial positions, this results in arbitrary variations for the NMSD. But observing the figures, the convergence has a clear tendency for the different cases.

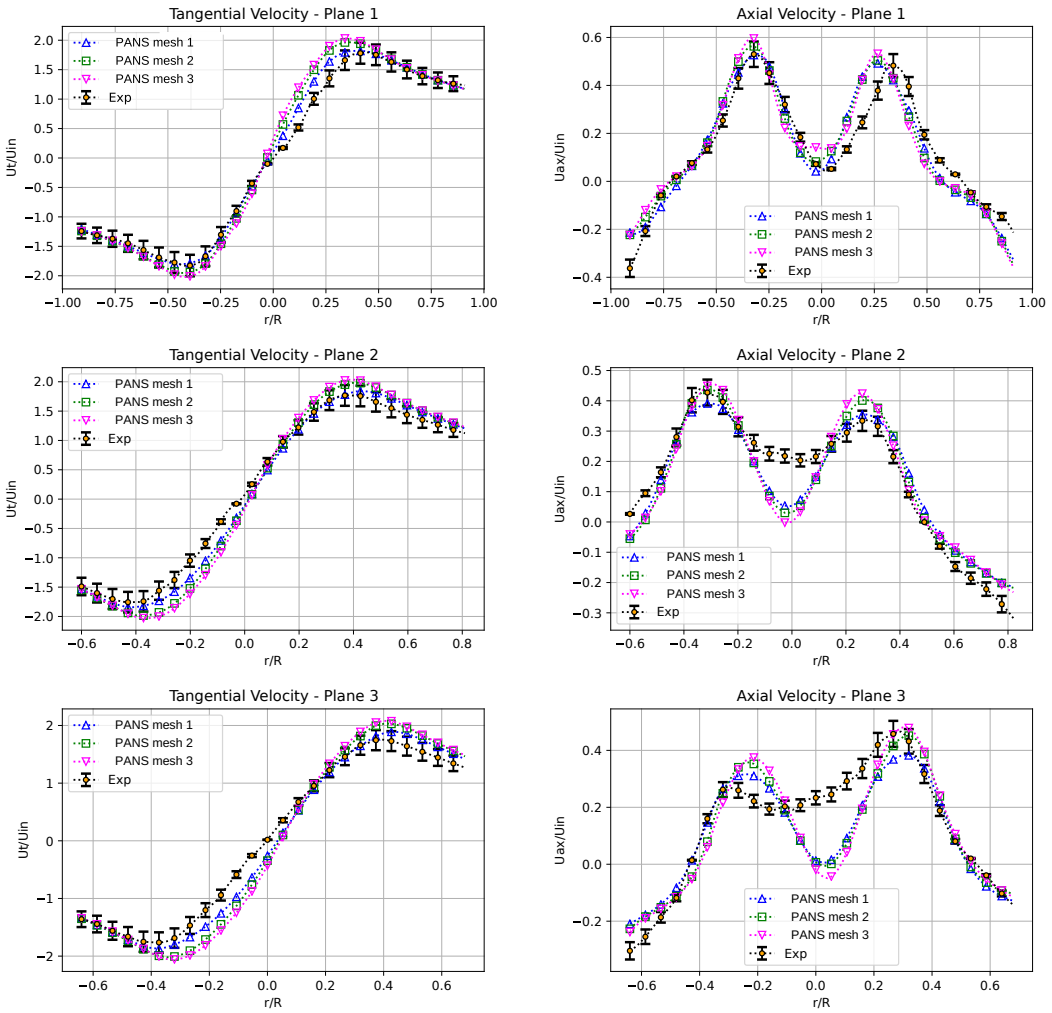

Figure 5. Radial distributions for the normalized mean tangential and axial velocities for the structured grids using the $k-\varepsilon$ PANS turbulence model.

3.3. *Mean velocity and mean pressure fields*

The mean tangential and axial velocity profiles are shown in Figure 7 in three different planes which are identical to those defined in the study of Jang et al. [15] (see Figure 1). For a valid comparison the structured mesh 3 with 1122544 cells was used, with the same discretization level as the mesh in the study of Jang et al. [15].

Figure 7 shows a comparison of the time averaged velocity profiles for the three different approaches (LES [15], RSM and $k-\varepsilon$ PANS). For the time-averaged tangential velocity profiles, the LES model has the smallest difference with respect to the experimental results in the 3 planes, while the $k-\varepsilon$ PANS model shows slightly higher differences with a 5.9% maximum deviation in plane 3 with respect to LES model.

For the axial velocity profiles, the RSM model shows the smallest differences with respect to the experimental results. The $k-\varepsilon$ PANS model is closer to LES results in the planes 1 and 3 with about 7.2% of maximum deviation in the plane 1. However, it is shown that PANS involve several

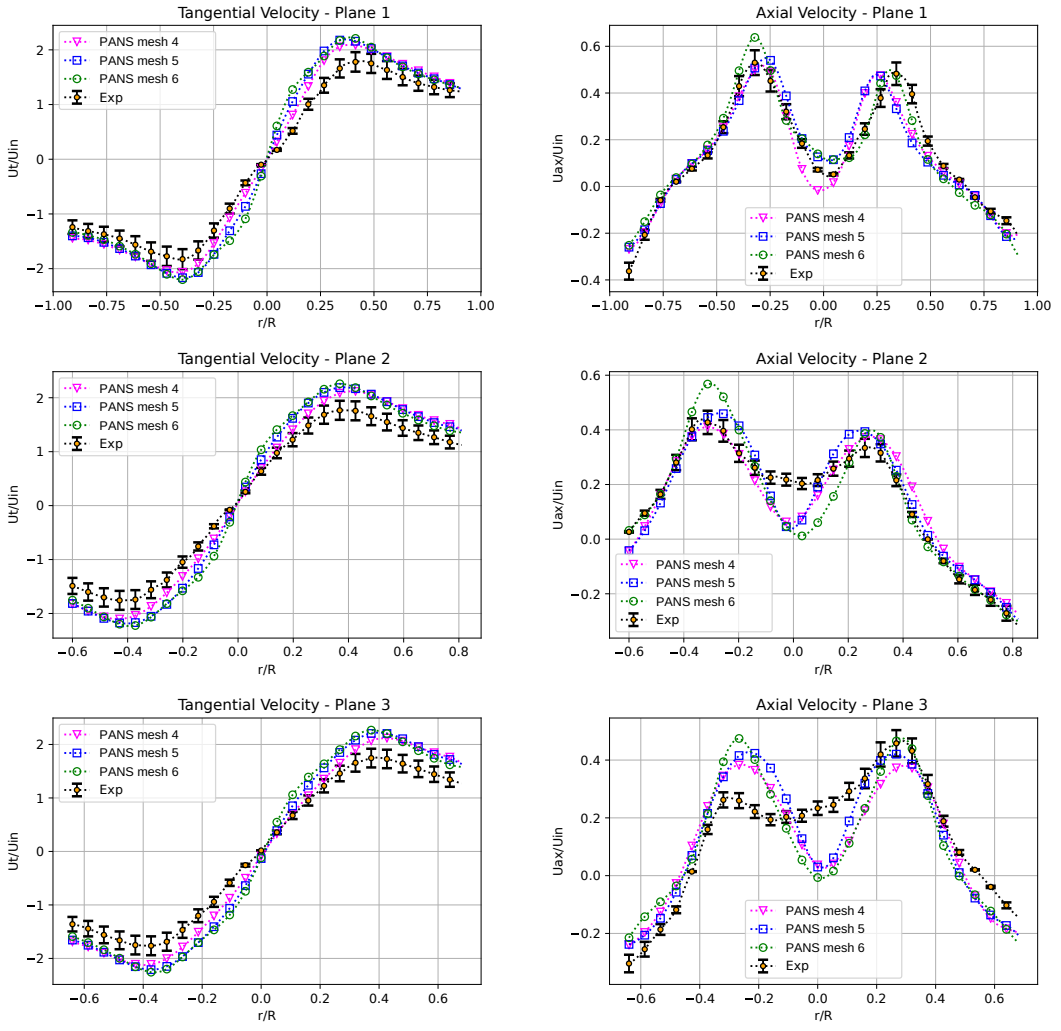

Figure 6. Radial distributions for the normalized mean tangential and axial velocities for the unstructured grids using the $k-\varepsilon$ PANS turbulence model.

discrepancies, especially on the tangential velocity (plane 1 and 3) and the local minimum of axial velocity at $r/R = 0$ (plane 2 and 3). Similar discrepancy can be observed for both others approaches, the local minimum of axial velocity which is overestimated by LES (plane 1) and underestimated for RSM (plane 2).

Figure 8 shows the time-averaged pressure fields distribution for the 3 models. For the PANS model, the pressure decreases radially towards the center and the precession of the vortex core is also observed like in the scalar field of the LES model, while for the RSM model the precession is hardly observed. The thickness of the vortex core is slightly smaller than the LES model, and this could be confirmed by comparing the distance between the two maximum velocity peaks for the axial and tangential velocities at the three planes. The depression at the core of the inner vortex is larger with PANS and RSM models than the LES model. Higher pressure values are also observed near the walls of the dust bin with the PANS model. The pressure drop across the cyclone was also determined by the same method as Jang et al. [15] in order to have a valid comparison.

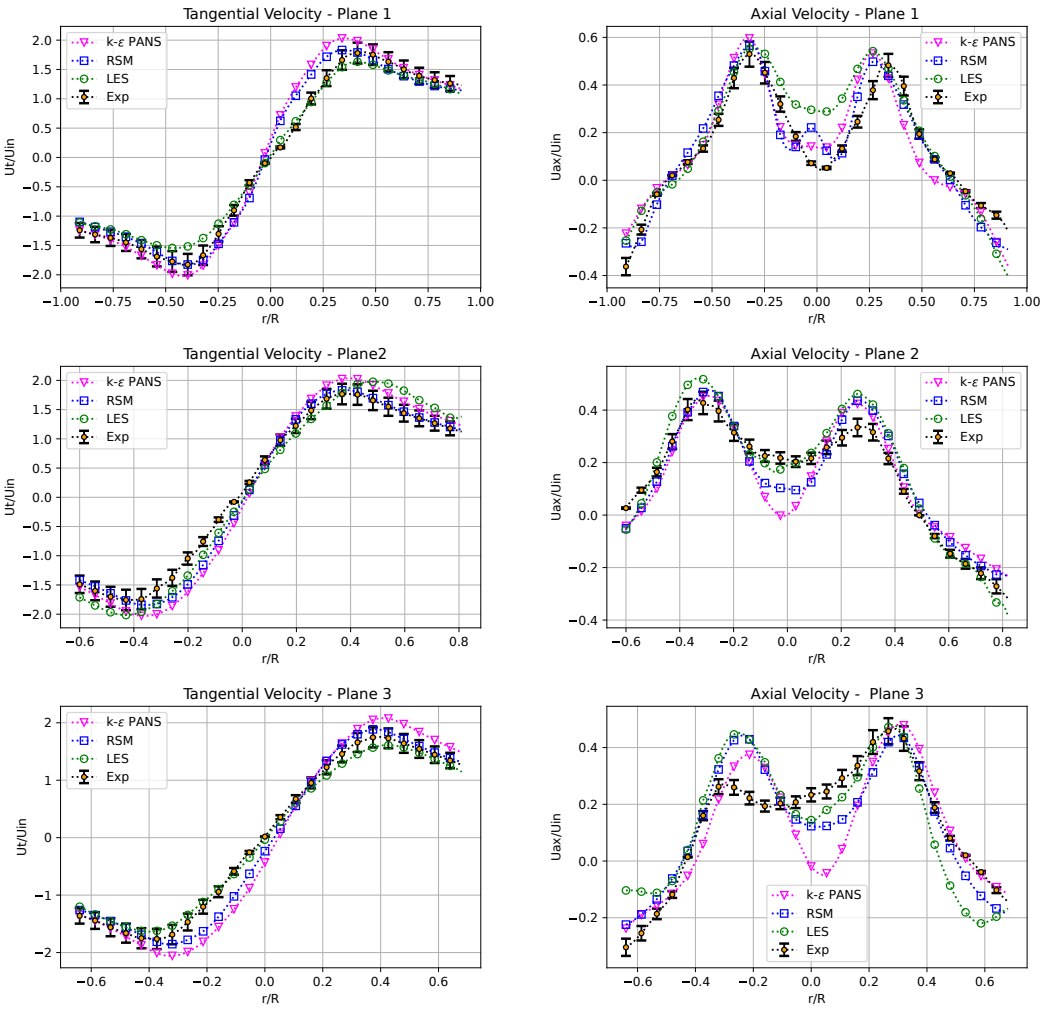

Figure 7. Radial distributions of the normalized mean tangential and axial velocities for the different turbulence models (LES [15], RSM and $k-\varepsilon$ PANS on mesh 3) with respect to the experimental results [4].

The PANS model predicts very accurately the pressure drop with approximately 1% of difference, meanwhile the other models have a pressure drop difference of approximately 11%.

The particles separation efficiencies are very sensitive to the velocity profiles, the tangential velocities governing the diffusion of the particles along the cyclone radius. The axial velocity leads the particles in the outward free vortex downward and towards the bin, and the finest particles towards the outlet by means of the inner forced-vortex.

Thus, a better prediction of these two components will result in a better prediction of the particles diffusion, and consequently a better prediction of the separation efficiencies. The accurate pressure field prediction will also result in a better estimation of the pressure forces on the particles as well as the pressure drop which characterizes the energy requirements for the operation of the cyclone. The PANS model globally shows acceptable results with respect to the two other models and the experimental results for both axial and tangential velocity profiles

and the pressure drop. It could be considered as the midway solution between RANS and LES approaches. It also resolves large turbulent structures, where the effect of turbulence on the particles will be represented more accurately, thus a more accurate prediction of the separation efficiency is expected.

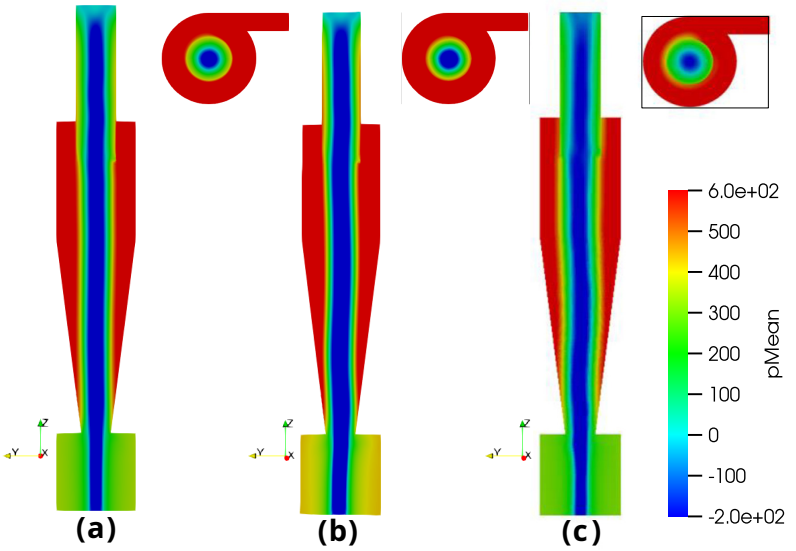

Figure 8. Comparison of the time-averaged pressure fields on mesh 3. (a): RSM, (b): PANS, (c): LES [15].

Figure 9 gives detailed information on the flow structure inside the cyclone. Many flow patterns were observed. In quadrant 1, a flow short circuit is established between the inlet and the vortex finder. This phenomenon is caused by the large recirculation zones formed due to the interactions between the external and internal vortices.These recirculation zones can be observed in the quadrants 2, 3 and 4, they also explain the precession phenomenon. The quadrant 4 shows the flow pattern inside the dust bin, the flow is expanded due to the expansion of the cross-section. The external vortex is also reversed due to its impact with the bin floor, creating the internal forced vortex.

3.4. *Computational time*

Execution time of the performed simulations are compared for 3 mesh sizes (mesh 1, 2 and 3) in Table 4. The compared time corresponds to the average of 1 second of simulation. The execution time for the $k-\varepsilon$ PANS model is considerably smaller than the RSM. It has 25% less execution time for 274k cells performed on 4 processors, and up to 74% for 589k cells performed on 8 processors. This model offers the middle ground between the accuracy and computational time, since the velocity profiles, the pressure drops are in good agreement with experimental results for considerably less computational time.

3.5. *Influence of the f_k parameter*

The parameter f_k allows the PANS method to shift between RANS, where $f_k = 1$, to DNS. To achieve that behavior, f_k is written as a specific ratio comparing the local grid size and the

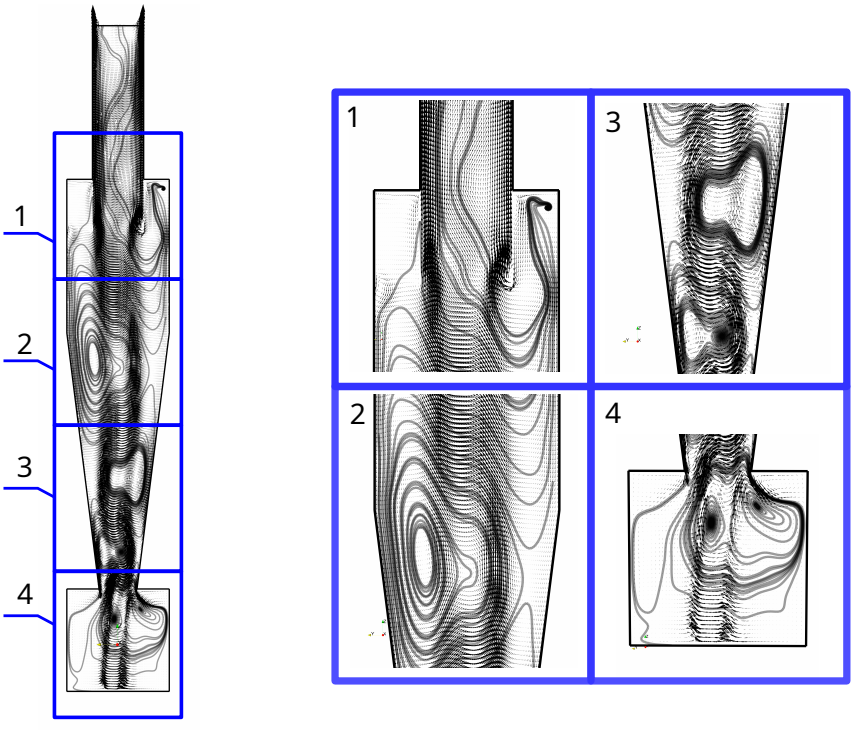

Figure 9. Averaged velocity streamlines (PANS, mesh 3) - Full view and zooms in different zones of the cyclone.

Table 4. Average execution time for one second of simulation for the $k-\varepsilon$ PANS and RSM models.

Execution time (s)			
model	mesh 1 (coarse)	mesh 2 (medium)	mesh3 (fine)
Procs. #	4	8	12
RSM	110 912	128 362	108 598
$k-\varepsilon$ PANS	82 610	71 704	85 023

local turbulent length scale. Recently, some studies [18, 26] focused on improving the original definition [1]. Here, only one new version is considered. The main goal is to determine if the PANS methodology used previously can still be improved. Indeed, the original equation (3) is known to give much too large turbulent viscosity which kills all resolved turbulence [18].

Velocity profiles are shown in Figure 10, NMSD results and pressure drop are summarized in Table 3. The simulation performed using the Davidson et al. f_k formulation (eq. (5)) shows a considerable enhancement in the prediction of the tangential and axial velocities with respect to the experimental results [4]. Equation (5) yield a slightly higher pressure drop difference (2.8% with respect to the experimental) but this difference is still satisfactory.

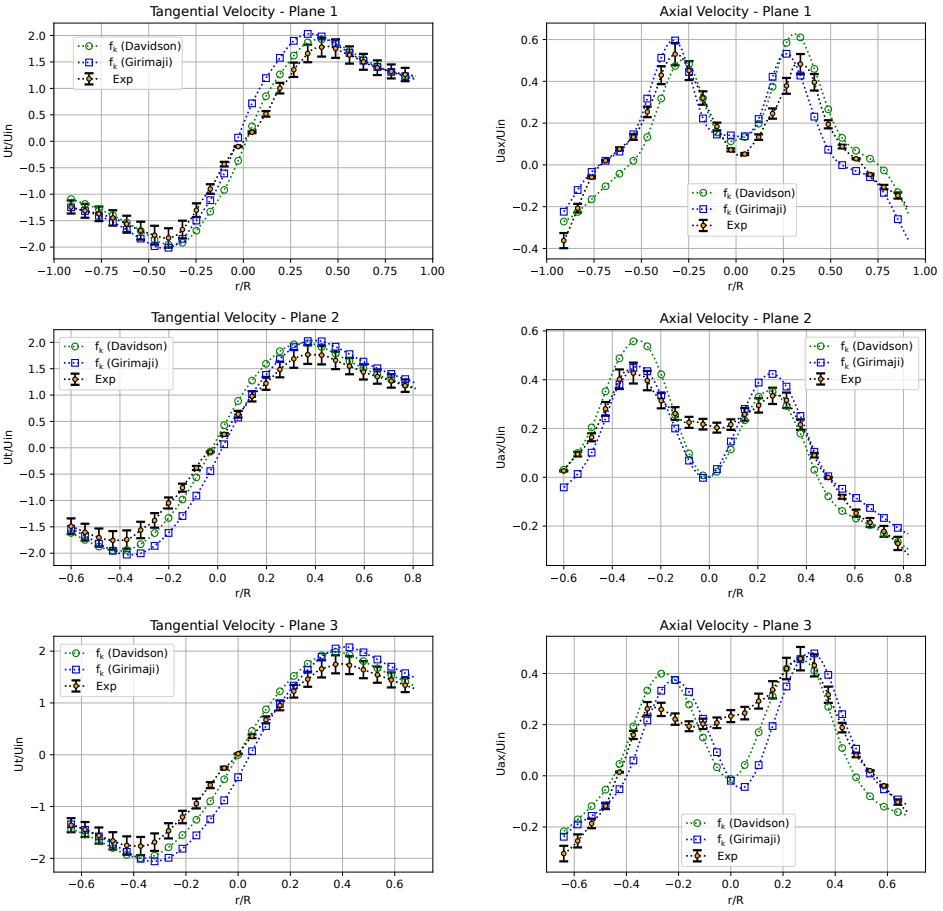

Figure 10. Comparison of velocity profiles with respect to the experimental results [4] for the $k-\varepsilon$ PANS using definitions (3) (Grimaji) and (5) (Davidson) on mesh 3.

3.6. *Influence of the mesh type on the results*

In this section, the comparison is done between a structured (mesh 3) and an unstructured (mesh 5) meshes that have almost the same number of cells. This test consists in evaluating the CPU time and the accuracy obtained to deduce the advantage of one type on another. The time averaged velocity profiles and the NMSD were compared to the experimental results [4] in the three reference planes, in addition to the pressure drop across the cyclone.

The structured mesh gave a better prediction of the tangential velocity profile in the three planes, with a maximum difference of 2.8% in plane 2. Meanwhile, for the axial component only the unstructured mesh gave smaller differences, with respect to experimental results, than the structured mesh in the three planes with a maximum difference between the two meshes of 4.3% in the plane 2. The unstructured mesh predicts poorly the pressure drop across the cyclone, with about 32% of difference with respect to the experimental value.

It is well known that the execution time for the unstructured mesh is more important than the one of the structured mesh. The latter one also offers a better prediction of the pressure drop and the tangential velocity profiles which have higher magnitudes than the axial component. They range from 0 to 2 times the inlet velocity. Meanwhile, the axial component have inferior

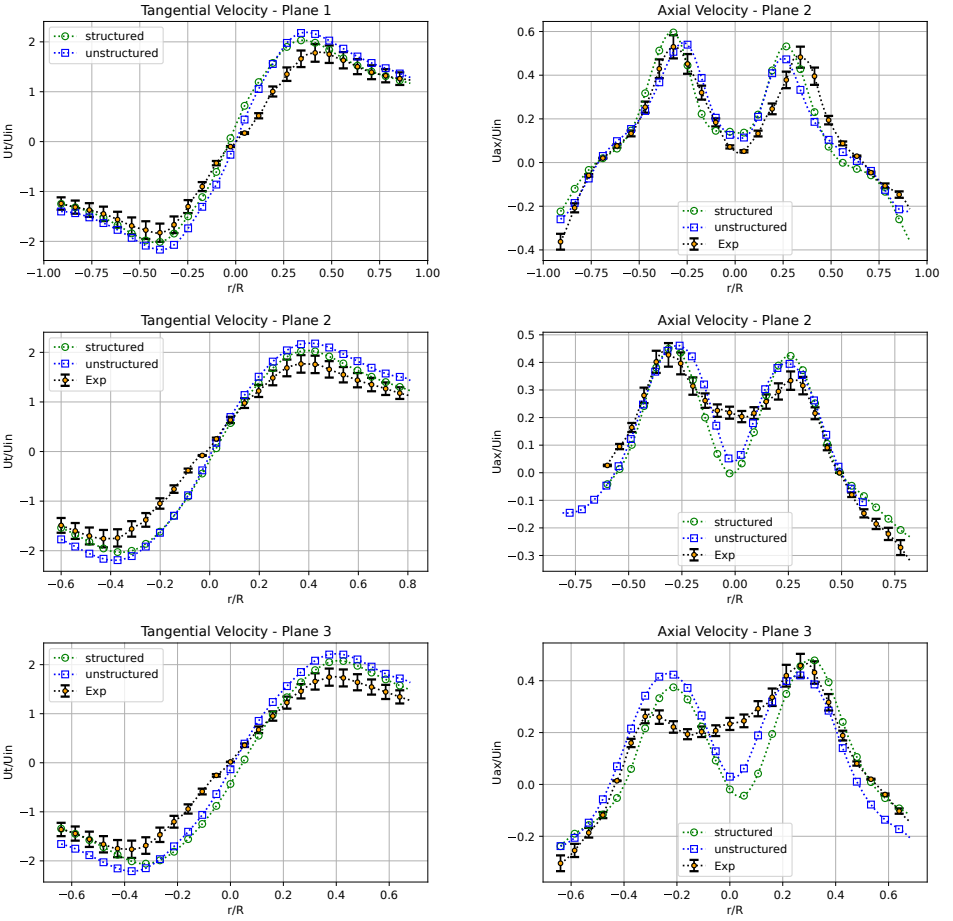

Figure 11. Experimental velocity profiles [4] compared to PANS results using structured (n°3) and unstructured (n°5) meshes.

magnitudes that reach at most 0.6 time the inlet velocity. This means that the differences of the tangential component are more weighted than the axial ones. But the structured meshes still have an important inconvenience which is the difficulty when it comes to generate it and especially when the geometries are more complex such as a cyclone that have circular inlet duct.

4. Conclusions

In the present work, the $k-\varepsilon$ PANS method is used to simulate the fluid flow inside a cyclone. The application of this model is evaluated in terms of accuracy and computation time, with respect to other turbulence models (LES, RSM) and different grid sizes and types. Two different definitions of the parameter f_k that precise the level of resolved quantities are also tested.

Several conclusions can be drawn :

- The $k-\varepsilon$ PANS predicts accurately the velocity profiles and especially the pressure drop compared to LES and RSM models.
- This model has a shorter computational time with respect to RSM. It is estimated to be around 22 % less for the finest mesh and 45% for the medium mesh.

- The f_k definition based on the Davidson's equation shows a better prediction of the velocity fields.
- The structured meshes offer a better prediction but they are still difficult to be generated. Especially, for PANS on structured meshes, the pressure drop differences with respect to the experimental value ranged from 0.5% to 1.1%.

Thus, using the PANS model with the Davidson's definition of the parameter f_k on a structured mesh could offer the best trade-off between accuracy and computational time for the simulation of industrial cyclones.

This approach represents a good potential for this industrial application, its main advantages being a good description of the anisotropy of the complex cyclone flow, excellent pressure drops prediction for a computational time which is lower than classical models often used for this type of application.

References

[1] S. S. Girimaji, K. Abdol-Hamid, "Partially Averaged Navier Stokes model for turbulence: Implementation and validation", in *43rd AIAA Aerospace Sciences Meeting and Exhibit*, 2005, p. 502.

[2] F. W. H. J. Boysan, W. H. Ayers, S. J., "A fundamental mathematical modelling approach to cyclone design", *Trans. Inst. Chem. Eng.* **60** (1982), no. 4, p. 222-230.

[3] P. Hadi Jafari, G. Hellström, R. Gebart, "Turbulence Modelling of a Single-Phase Flow Cyclone Gasifier", *Engineering* **9** (2017), no. 9, p. 779-799.

[4] A. J. Hoekstra, J. J. Derksen, H. E. A. Van Den Akker, "An experimental and numerical study of turbulent swirling flow in gas cyclones", *Chem. Eng. Sci.* **54** (1999), no. 13-14, p. 2055-2065.

[5] D. Bogdanov, S. Poniaev, "Numerical simulation of turbulent flow in a cyclonic separator", *J. Phys., Conf. Ser.* **572** (2014), no. 1, article no. 012056.

[6] B. Wang, D. L. Xu, K. W. Chu, A. B. Yu, "Numerical study of gas-solid flow in a cyclone separator", *Appl. Math. Modelling* **30** (2006), no. 11, p. 1326-1342.

[7] T. G. Chuah, J. Gimbun, T. S. Y. Choong, "A CFD study of the effect of cone dimensions on sampling aerocyclones performance and hydrodynamics", *Powder Technol.* **162** (2006), no. 2, p. 126-132.

[8] B. Zhao, Y. Su, J. Zhang, "Simulation of gas flow pattern and separation efficiency in cyclone with conventional single and spiral double inlet configuration", *Chem. Eng. Res. Des.* **84** (2006), no. 12, p. 1158-1165.

[9] H. Zhou, Z. Hu, Q. Zhang, Q. Wang, X. Lv, "Numerical study on gas-solid flow characteristics of ultra-light particles in a cyclone separator", *Powder Technol.* **344** (2019), p. 784-796.

[10] F. Kaya, I. Karagoz, A. Avci, "Effects of surface roughness on the performance of tangential inlet cyclone separators", *Aerosol Sci. Technol.* **45** (2011), no. 8, p. 988-995.

[11] M. He, Y. Zhang, L. Ma, H. Wang, P. Fu, Z. Zhao, "Study on flow field characteristics in a reverse rotation cyclone with PIV", *Chem. Eng. Process.* **126** (2018), p. 100-107.

[12] E. Balestrin, R. K. Decker, D. Noriler, J. C. S. C. Bastos, H. F. Meier, "An alternative for the collection of small particles in cyclones: Experimental analysis and CFD modeling", *Sep. Purif. Technol.* **184** (2017), p. 54-65.

[13] L. S. Brar, R. P. Sharma, K. Elsayed, "The effect of the cyclone length on the performance of Stairmand high-efficiency cyclone", *Powder Technol.* **286** (2015), p. 668-677.

[14] K. Elsayed, C. Lacor, "The effect of vortex finder diameter on cyclone separator performance and flow field", in *ECCOMAS CFD Conf., JCF Pereira and A. Sequeira (Eds.) Lisbon*, 2010.

[15] K. Jang, G. G. Lee, K. Y. Huh, "Evaluation of the turbulence models for gas flow and particle transport in URANS and LES of a cyclone separator", *Comput. Fluids* **172** (2018), p. 274-283.

[16] K. Elsayed, C. Lacor, "The effect of cyclone vortex finder dimensions on the flow pattern and performance using LES", *Comput. Fluids* **71** (2013), p. 224-239.

[17] G. Gronald, J. J. Derksen, "Simulating turbulent swirling flow in a gas cyclone: A comparison of various modeling approaches", *Powder Technol.* **205** (2011), no. 1-3, p. 160-171.

[18] H. Foroutan, S. Yavuzkurt, "A partially-averaged Navier–Stokes model for the simulation of turbulent swirling flow with vortex breakdown", *Int. J. Heat Fluid Flow* **50** (2014), p. 402-416.

[19] S. Lakshmipathy, S. S. Girimaji, "Extension of Boussinesq turbulence constitutive relation for bridging methods", *J. Turbul.* (2007), no. 8, article no. N31.

[20] M. Breuer, "A challenging test case for large eddy simulation: high Reynolds number circular cylinder flow", *Int. J. Heat Fluid Flow* **21** (2000), no. 5, p. 648-654.

[21] B. Cantwell, D. Coles, "An experimental study of entrainment and transport in the turbulent near wake of a circular cylinder", *J. Fluid Mech.* **136** (1983), p. 321-374.
[22] D. M. Driver, H. L. Seegmiller, J. G. Marvin, "Time-dependent behavior of a reattaching shear layer", *AIAA J.* **25** (1987), no. 7, p. 914-919.
[23] B. Basara, S. Krajnović, S. S. Girimaji, "PANS vs. LES for computations of the flow around a 3D bluff body", in *Proc. of ERCOFTAC 7th Int. Symp.-ETMM7, Lymassol, Cyprus*, vol. 2, 2008, p. 3.
[24] X. Han, S. Krajnović, B. Basara, "Study of active flow control for a simplified vehicle model using the PANS method", *Int. J. Heat Fluid Flow* **42** (2013), p. 139-150.
[25] B. Basara, S. Krajnović, Z. Pavlovic, P. Ringqvist, "Performance analysis of Partially-Averaged Navier-Stokes method for complex turbulent flows", in *6th AIAA Theoretical Fluid Mechanics Conference*, 2011.
[26] L. Davidson, C. Friess, "A new formulation of fk for the PANS model", *J. Turbul.* **20** (2019), no. 5, p. 322-336.
[27] K. Elsayed, C. Lacor, "Numerical modeling of the flow field and performance in cyclones of different cone-tip diameters", *Comput. Fluids* **51** (2011), no. 1, p. 48-59.
[28] P. J. Roache, "Quantification of uncertainty in computational fluid dynamics", *Annu. Rev. Fluid Mech.* **29** (1997), no. 1, p. 123-160.